Bursting events in zonal flow-drift wave turbulence

G. Manfredi and C. M. Roach

Citation: Phys. Plasmas **10**, 2824 (2003); doi: 10.1063/1.1581284
View online: http://dx.doi.org/10.1063/1.1581284
View Table of Contents: http://pop.aip.org/resource/1/PHPAEN/v10/i7
Published by the American Institute of Physics.

Bursting events in zonal flow-drift wave turbulence

G. Manfredi
Laboratoire de Physique des Milieux Ionisés et Applications, CNRS-Université H. Poincaré, BP 239, 54506 Vandoeuvre-les-Nancy, France

C. M. Roach
Euratom/UKAEA Fusion Association, Culham Science Centre, Abingdon, Oxfordshire, United Kingdom

(Received 21 February 2003; accepted 15 April 2003)

The generation of zonal flows and their interplay with drift wave turbulence is studied numerically using a model based on the Hasegawa–Mima equation, with an electron response depending only on the fluctuating part of the electrostatic potential. In regimes dominated by the diamagnetic velocity, large-amplitude nonlinear oscillations are observed in the time history of the zonal flow and drift wave spectra. Such oscillations have also recently been detected in toroidal gyrokinetic simulations, and could be important in determining the transport behavior in experimental devices.
 [DOI: 10.1063/1.1581284]

I. INTRODUCTION

Drift waves (DWs) play an important role in the physics of strongly magnetized plasmas. When unstable, such as in the presence of sufficiently steep temperature gradients, they can give rise to fully developed ''drift'' turbulence, which is considered a likely candidate to explain the anomalous transport rates observed in present tokamaks. It is widely believed that ''zonal flows'' (ZFs) (i.e., modes that only depend on the radial coordinate) are a crucial factor in regulating the nonlinear evolution of drift-wave instabilities, such as the ion temperature gradient (ITG) instability, and consequently the level of turbulent transport. Zonal flows can also have an impact on radially elongated, poloidally localized structures (''streamers''), which are thought to generate large-scale events (bursts) in tokamak plasmas[1–3] thereby leading to long-range correlations and possibly nondiffusive transport.[4,5]

Several theoretical models, based on the Hasegawa–Mima equation,[6] have been proposed in order to explain the emergence of ZFs in tokamak plasmas.[7–12] The simplest model involves the modulational instability of a monochromatic drift wave (the pump), generating two sidebands and a ZF that finally saturate by depletion of the pump wave.[9–12] However, models involving only a small number of waves cannot describe correctly the broad-band turbulence occurring in tokamak experiments and simulations. In particular, a distinct feature recently observed in several large-scale numerical simulations is the appearance of ''bursts,'' i.e., punctuated events during which radial transport is considerably enhanced. In ITG turbulence and in resistive ballooning turbulence,[2,3,13] it has been observed that such bursts occur at times of low zonal flow activity, whereas, conversely, high zonal flow activity corresponds to periods of significantly lower transport. This mechanism yields a characteristic oscillatory pattern in the DW-ZF dynamics.

In order to explain this complex behavior, Malkov and co-workers[14] have derived a simplified ''predator–prey'' system that mimics the nonlinear interplay of DWs and ZFs. Although more realistic than previous four-wave models, it is, however, still based on a number of crucial assumptions, namely (a) it relies on a Vlasov-type equation for the wave actions (weak turbulence) rather than on a first-principles based turbulence model; (b) rapidly varying and short wavelength scales are averaged over in order to obtain a one-dimensional (radial) equation in wave number space. On the other hand, the numerical results of Lin *et al.*[13] are obtained from three-dimensional full-torus gyrokinetic simulations. Given the complexity of large codes, such simulations can follow the dynamics only over a few oscillation periods and for a small set of relevant parameters. In addition, the number of physical effects potentially at play is very large, making it difficult to sort out which of them is the essential ingredient. Bursty transport has also been discovered and studied in fluid models of particular instabilities (resistive ballooning modes and ITG drift waves),[2,3] where it is linked to the appearance of radially elongated structures known as streamers.

It is useful to attempt to fill the gap between the predator–prey model and the global gyrokinetic simulations, using direct drift turbulence simulations based on a simpler and more tractable two-dimensional slab model. The results from such simulations can be used to verify and strengthen our confidence in the intuitive (but simplified) picture of Malkov,[14] and help to isolate the key model ingredients which are responsible for these effects in the more realistic (but complex) simulations of Lin *et al.*[13]

II. MODEL

The model used here is the one adopted by Smolyakov *et al.*[7,8] to describe the dynamics of drift waves in the poloidal plane. It is essentially a Hasegawa–Mima (HM) equation,[15] with an adiabatic electron response modified so that the electron density fluctuation is independent of the flux-surface-averaged part of the electrostatic potential.[16] In the two-dimensional slab geometry used in this paper, x is the poloidal coordinate and y is the radial coordinate (note

that this convention is not the one commonly used in fusion theory). The electrostatic potential can be represented as the sum of a flux-surface averaged value $\overline{\phi}(y,t)$ (the zonal flows) and a contribution which varies on a flux surface $\tilde{\phi}(x,y,t)$ (the drift waves), where

$$\overline{\phi}(y,t)=\int_0^a \phi(x,y,t)dx$$

and where a is the poloidal slab size. ZFs are defined as modes for which $k_x=0$, and DWs as modes with $k_x\neq 0$.

We use dimensionless "large-scale" units, by normalizing space to the box size a, time to $1/(\omega_{ci}\rho_*^2)$, and the electric potential to T_e/e. We have defined $\rho_*=\rho_s/a$, where $\rho_s=\sqrt{T_e m_i}/eB$ is the ion thermal Larmor radius evaluated at the electron temperature, and $\omega_{ci}=eB/m_i$ is the ion cyclotron frequency. In these units, the modified Hasegawa–Mima equation of Ref. 11 can be written as

$$\frac{\partial w}{\partial t}+\{\phi,w\}+\beta\frac{\partial \phi}{\partial x}=F-D, \tag{1}$$

where $w=\phi-\overline{\phi}-\rho_*^2\nabla_\perp^2\phi$ is the potential vorticity, and the Poisson bracket $\{\cdot,\cdot\}$ represents the convection due to the $\mathbf{E}\times\mathbf{B}$ flow. F and D are the normalized forcing and dissipation terms that will be described shortly. Boundary conditions are taken to be periodic in both directions, with spatial period equal to a (which represents a macroscopic length scale, such as the minor radius, in the tokamak configuration). We have also defined $\beta=a/L_n$, where L_n is the characteristic length scale of the plasma density gradient.

The standard HM model[15] is formally identical to Eq. (1), but with the potential vorticity field defined as $w=\phi-\rho_*^2\nabla_\perp^2\phi$. This reflects the fact that, in the standard HM model, electrons are allowed to thermalize *across* magnetic surfaces; such unphysical behavior is forbidden in the modified HM model.

In order to achieve steady-state turbulence, forcing and dissipation terms should also be implemented. The dissipation consists of two terms: $D=D_1+D_2$. The first affects both the DW and the ZF components of the potential and has the form $D_1=\mu_1\rho_*^2|\nabla_\perp|^{2p}\phi$: it represents a hyperdiffusion term as frequently adopted in fluid simulations in order to restrict dissipation to the smallest scales; it reduces to standard diffusion for $p=2$. The second term acts only on the ZFs (Ref. 17) and can be written as $D_2=-\mu_2\rho_*^2\nabla_\perp^2\overline{\phi}$. The constants $\mu_{1,2}$ are dimensionless dissipation coefficients. The D_2 term ensures that large scale ZFs are ultimately damped. Indeed, in toroidal geometry, ZFs are damped by collisionless transit time magnetic pumping effects.[13,18] In our case, it is easy to show, using the above dissipative terms, that the total damping rate for the ZF is $\Gamma_k^{\mathrm{ZF}}=\mu_2+\mu_1 k^{2p-2}$ (plotted in Fig. 1), which does not vanish as $k\to 0$.

We have adopted a forcing term which is isotropic in wave number space for the DW modes, and has the form of an instability which can be expressed in wave number space as $F_{\mathbf{k}}=\gamma(k)w_{\mathbf{k}}$. The growth rate $\gamma(k)$ depends only on the magnitude of the wave number, and is peaked around a given wave number k_0,

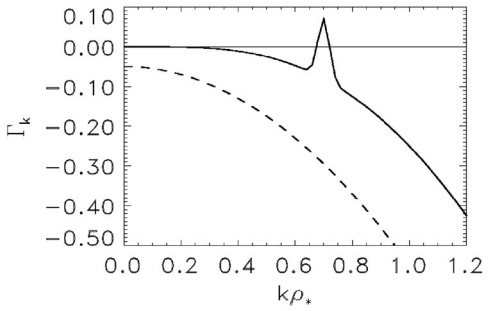

FIG. 1. Total linear rate (growth minus dissipation) for the DWs (solid line) and the ZFs (dashed line), as a function of the radial wave number. The parameters are those specified in Sec. III A, with, in addition, $\mu_2=0.05$.

$$\gamma(k)=\gamma_0\exp\left(-\frac{(k-k_0)^2}{2\sigma^2}\right), \tag{2}$$

where γ_0 is the maximum growth rate (corresponding to k_0), and σ is the band width. This term mimics an instability such as ITG, which normally peaks at wave numbers $k_0\rho_s$ of order unity or lower.[19] For ZFs, the forcing term is set to zero, as these modes are generally linearly stable. The total linear rate (growth minus damping) is plotted in Fig. 1 for both ZFs and DWs, for the case studied in Sec. III A. Note that only a small band of wave numbers are linearly unstable, and that ZFs are more strongly damped than DWs for all values of k.

We also point out that the forcing rate γ_0 can always be eliminated by a suitable rescaling transformation. Therefore, our model contains four independent dimensionless parameters: the thermal Larmor radius ρ_*, the ratio a/L_n (related to the density gradient), and the normalized viscous coefficients μ_1/γ_0, μ_2/γ_0. In addition, one must consider the shape of the forcing function, which in Eq. (2) is parameterized by a peak wave number k_0 and a bandwidth σ.

Finally, we note that instability growth rates are assumed to be constant in our model, although in principle they are sensitive to several parameters, such as the local density gradient L_n^{-1}. The normalized damping coefficients $\mu_{1,2}/\gamma_0$ (which govern the appearance of large oscillations) may therefore depend on the instability model, and this fact should be borne in mind when interpreting the results presented in the next section.

III. RESULTS

Equation (1) is solved numerically using a pseudospectral method[11] with full dealiasing. The time-stepping is performed with an explicit leapfrog technique, with a predictor–corrector scheme applied at regular intervals (every ~ 50 time steps). The overall scheme is second order accurate in time. In all calculations the grid dimensions in the x and y directions are given by $N_x=N_y=256$ (after dealiasing), and the time step typically varies in the range 0.0025–0.01.

A. Effect of poloidal flow damping

The parameters of all the runs reported in this paper are summarized in Table I. Here we present results obtained for the following set of dimensionless parameters: $\rho_*=0.02$, β

TABLE I. Summary of the parameters used in the runs of Secs. III A–III C.

	III A	III B	III C
ρ_*	0.02	0.02	0.007
β	1.0	0.–0.3–0.8–2.	0.–1.–5.
p	2	2	4
μ_1	2×10^{-4}	2×10^{-4}	2×10^{-12}
μ_2	0.–0.1–0.25–1.	0.05	0.05
γ_0	0.15	0.15	1.25
$\rho_* k_0$	0.7	0.7	0.7
σ	1.0	1.0	1.0

$=a/L_n=1$, $\mu_1=2\times10^{-4}$, $p=2$, $\gamma_0=0.15$, $\rho_* k_0=0.7$, and $\sigma=1$. The ZF damping rate has been varied from $\mu_2=0$ to $\mu_2=1.0$ in order to allow comparison with the results of Ref. 14. At $t=0$, the electrostatic potential is initialized as a bath of waves with random phases and very low amplitude. In the initial stages of the evolution, DW modes with a positive growth rate start growing exponentially. When the DW spectrum has reached a certain amplitude, the ZF modes are excited and also grow exponentially, with a larger growth rate with respect to the DWs [Fig. 2(a)]. The observed growth rate for the DWs is $\gamma_{\mathrm{DW}}\simeq0.065$, which corresponds to the net rate (growth minus dissipation) of modes with $\rho_* k=0.7$ (see Fig. 1). For ZFs, we obtain a growth rate $\gamma_{\mathrm{ZF}}\simeq0.13$, which is approximately twice the observed DW growth rate. In these runs, the faster-than-exponential growth reported in Ref. 1 was not observed.

We have found that the observed ZF growth rate is insensitive to the value of the ZF damping, μ_2 [Fig. 2(b)]. The

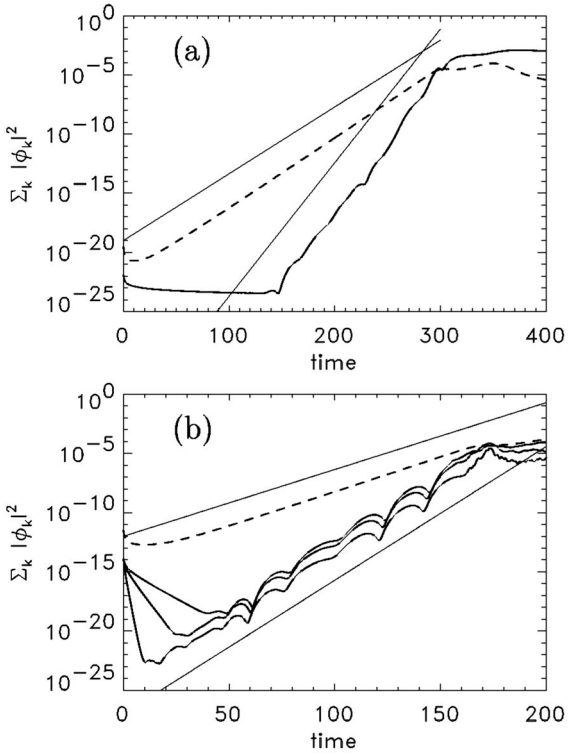

FIG. 2. Early time evolution of the ZF (solid line) and DW (dashed line) spectrum (a) for $\mu_2=0$, and (b) for $\mu_2=0.1$, 0.25, and 1.0. The straight lines correspond to growth rates $\gamma=0.13$ and 0.065.

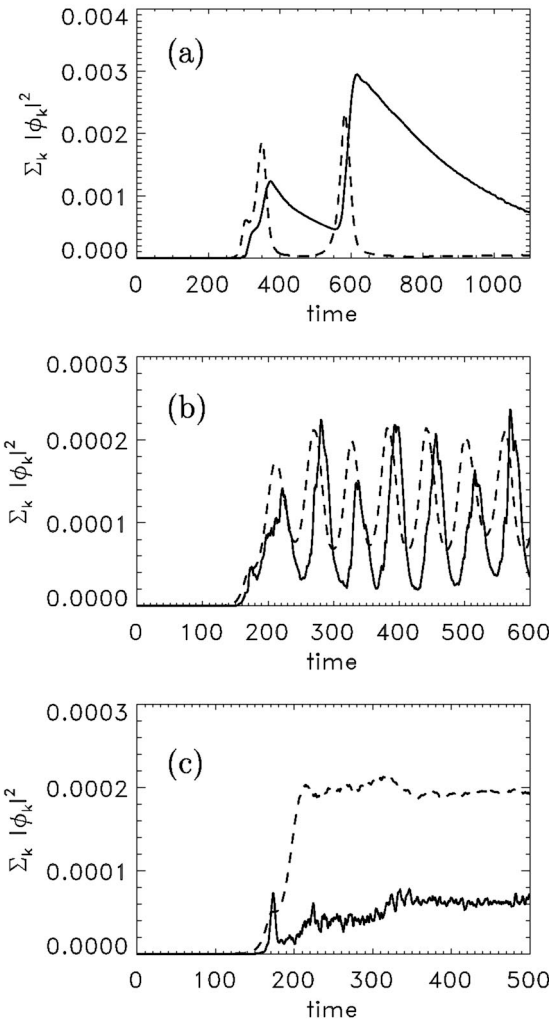

FIG. 3. Time evolution of the ZF (solid line) and DW (dashed line) spectra, for (a) $\mu_2=0.0$, (b) $\mu_2=0.10$, and (c) $\mu_2=0.25$. For clarity, the DW spectrum in (a) is magnified by a factor 20.

fact that $\gamma_{\mathrm{ZF}}\simeq2\gamma_{\mathrm{DW}}$ (independent of the ZF damping) is entirely due to the quadratic nature of the nonlinearity. Each ZF mode evolves under the action of at least one pair of DW modes, with each coupling forming a triad in wave vector space and schematically obeying an equation of the type,[11]

$$\frac{d\phi_{\mathrm{ZF}}}{dt}=K\ \phi_1\phi_2-\eta\phi_{\mathrm{ZF}}, \tag{3}$$

where $\phi_{1,2}(t)=A_{1,2}\exp(\gamma_{\mathrm{DW}}t)$ are two DW modes, η is a dissipation rate (related to our μ_2 coefficient), and K is a coupling coefficient. This equation has the general solution:

$$\phi_{\mathrm{ZF}}(t)=\frac{KA_1A_2}{2\gamma_{\mathrm{DW}}+\eta}\exp(2\gamma_{\mathrm{DW}}t)+c\ \exp(-\eta t), \tag{4}$$

where c is an integration constant. The first term in Eq. (4) grows to dominate the solution, and determines that the ZF growth rate is twice that of the DWs independent of η, entirely consistent with the simulation results.

After saturation of the instability, an oscillating regime takes place (Fig. 3). The evolution of the ZF and DW amplitudes is plotted in Figs. 3(a)–3(c) for three values of the ZF

damping rate μ_2. For $\mu_2=0$ [Fig. 3(a)] the DW spectrum displays a narrow peak followed by a sharp decay; the ZF spectrum peaks with a time lag with respect to the DW, and then decays much more slowly. Note that the ZF *growth rate* is maximum when the DW spectrum peaks, whereas the DW *decay rate* is maximum when the ZF spectrum peaks. This behavior is close to Malkov *et al.*'s type (3) behavior,[14] which corresponds to a case of zero ZF damping. In a broadband simulation such as ours, some dissipation must necessarily be present (the total ZF damping rate here is $\Gamma_k^{ZF}=\mu_1 k^2$), so that the ZF spectrum still decays, albeit slowly. In this regime, even though some DW modes are linearly unstable, they give rise to an extremely low level of steady-state turbulence, as the latter is completely suppressed by the ZFs. This effect is known as the Dimits upshift of the turbulence threshold.[20]

Increasing the ZF damping rate to $\mu_2=0.1$ yields the oscillatory behavior shown in Fig. 3(b), again with a time lag between the ZF and DW peaks. This behavior is similar to the type (2) behavior described by Malkov *et al.*[14] (quasi-periodic bursting). No significant decay of the oscillations was observed by extending the run up to times as long as $t=1000$. When the ZF damping is even stronger [$\mu_2=0.25$, Fig. 3(c)], both the ZF and DW modes saturate at a roughly constant level, with small fluctuations. By performing other simulations, we found that the large amplitude oscillations are virtually suppressed for $\mu_2>0.15$. Notice that the switch between the two behaviors (with and without oscillations) is very sudden.

The oscillatory behavior was explained by Malkov *et al.*[14] in terms of a ''predator–prey'' model, where the DWs correspond to the ''prey'' and the ZFs to the ''predator.'' In our system the DWs grow due to the imposed growth rate, and when they attain a sufficient amplitude the ZFs also start to grow, feeding off the DWs through the nonlinear coupling term. Then, when the ZFs reach a sufficiently large amplitude, the DWs start to be diminished by the shearing effect of the poloidal rotation associated with the ZFs. The source of ZFs is thus reduced as the DWs diminish (i.e., the predators ''starve''). When the ZFs reach a sufficiently low amplitude, the DWs can begin to grow again, and so the whole cycle repeats. This simple model explains the $\pi/2$ phase shift observed in the DW and ZF oscillations.

The ZF saturation amplitude can qualitatively be estimated by equating the two terms on the right-hand side (RHS) of Eq. (3),

$$\phi_{ZF}\sim K\phi_1\phi_2/\eta. \tag{5}$$

Naturally, this predicts that the ZF saturation amplitude reduces with increasing dissipation (although their growth rate stays the same), and this is clearly observed in the long-time results presented in Fig. 3.

Figure 4 shows the DW isotropic potential spectrum for the run with $\mu_2=0.1$ at two different times, corresponding respectively to a peak and a depression in the DW evolution of Fig. 3(b). We notice that the spectrum is relatively broad, and rather flat for low wave numbers. A significant number of DW modes are therefore excited.

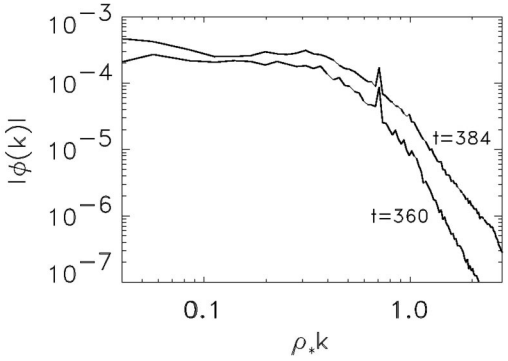

FIG. 4. DW spectrum at two different times corresponding to a peak ($t=384$) and a depression ($t=360$) in the DW evolution of Fig. 3(b).

In the standard HM model, cross-field electron flows arising from the adiabatic electron response suppress the growth of ZF modes. Such electron flows are unphysical, and are not present in the modified HM model. However, if the ZF damping rate is very large, the ZFs should be suppressed very efficiently even in the modified HM model. In that case, we should expect the dynamics to approach that of the standard HM equation. In order to verify this fact, we have performed a simulation with $\mu_2=1$ and compared it with a standard HM case (Fig. 5). As expected, the level of saturation of the DW is very similar in the two runs [Fig. 5(a)], and much larger than that of the ZF. The evolution of the ZFs is shown in Fig. 5(b) on a logarithmic scale; for the standard HM run, the zonal flows also grow exponentially with the

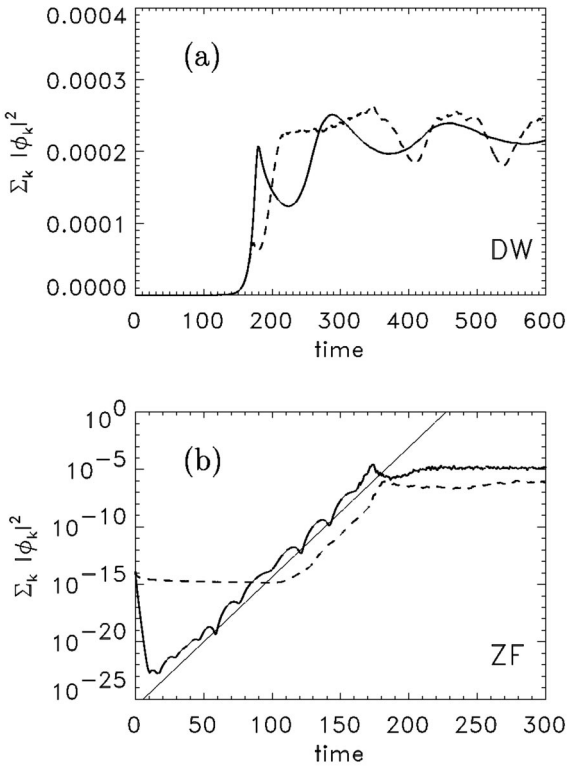

FIG. 5. Time evolution (a) of the DWs and (b) of the ZFs. The standard HM results are presented as dashed lines and the modified HM results with $\mu_2=1$ as solid lines. The straight line in (b) corresponds to a growth rate $\gamma=0.13$.

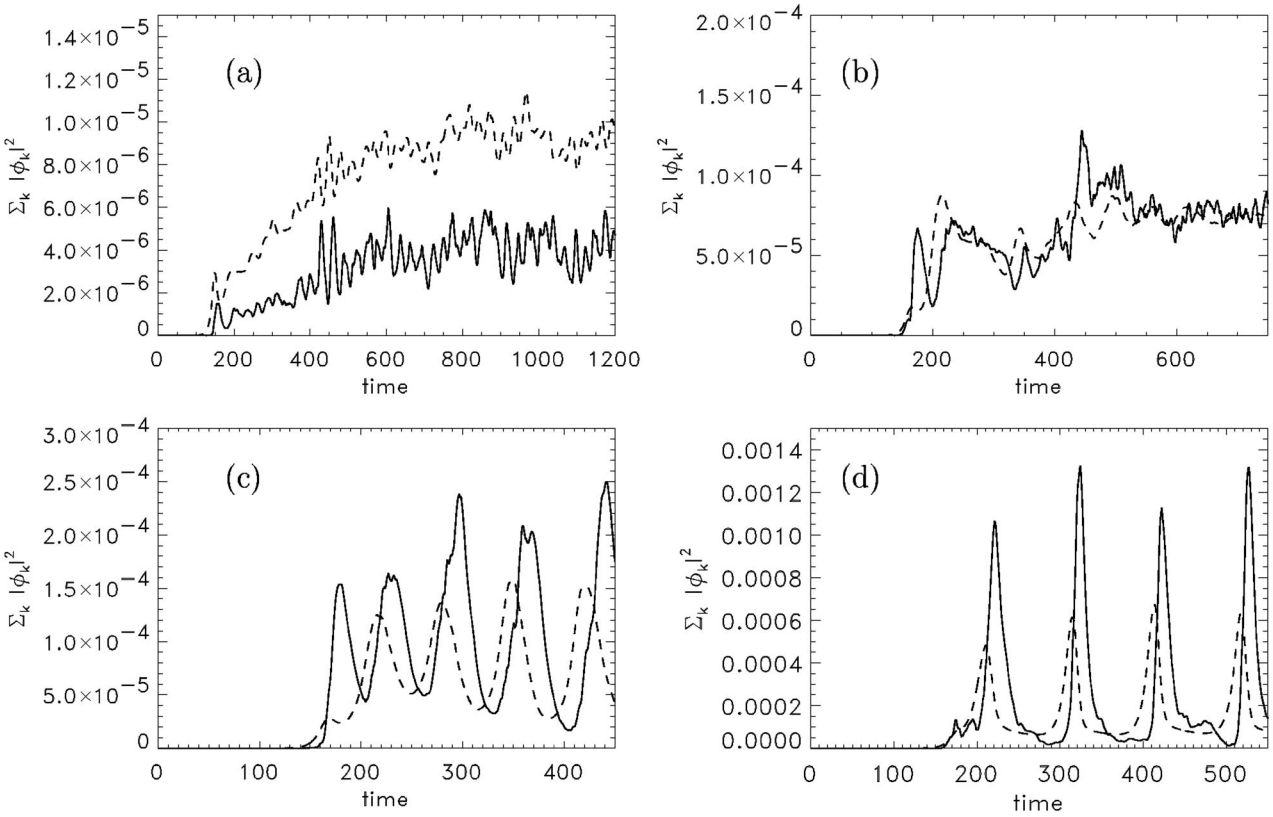

FIG. 6. Time evolution of the ZF (solid line) and DW (dashed line) spectra (Sec. III B), (a) for $\beta=0$, (b) for $\beta=0.6$, (c) for $\beta=0.8$, and (d) for $\beta=2.0$.

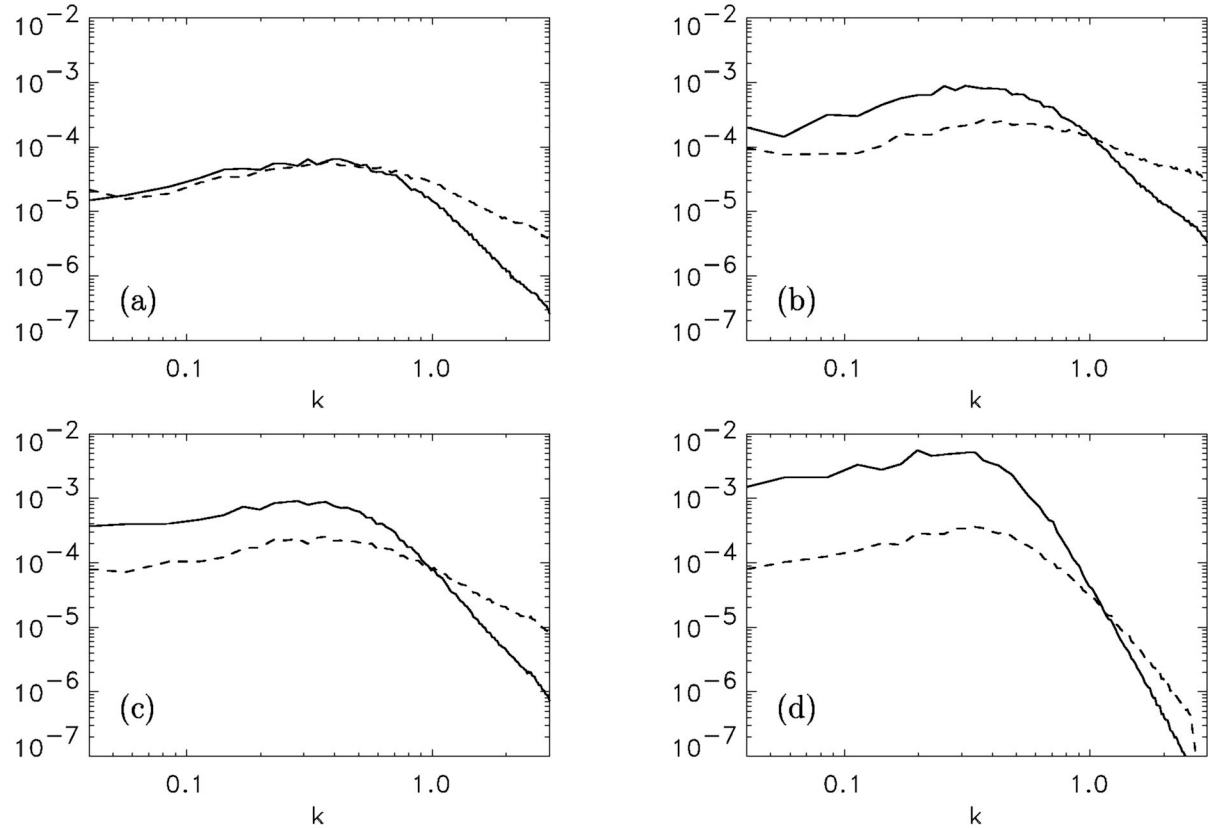

FIG. 7. Isotropic DW spectrum of the linear diamagnetic term (solid line) and the nonlinear term (dashed line), for (a) $\beta=0.1$, (b) $\beta=0.6$, (c) $\beta=0.8$, and (d) $\beta=2.0$.

same rate ($\gamma_{ZF} \simeq 0.13$) as for the modified HM equation, which is consistent with the previous discussion showing that $\gamma_{ZF} = 2\gamma_{DW}$ independently of all other parameters. On the other hand, the ZF saturation level does depend on the constant K [see Eq. (5)], which couples nonlinearly wave vectors $\mathbf{k}_1$ and $\mathbf{k}_2$ to generate wavevector $\mathbf{k}_{ZF}$. This coupling constant can be written as[11]

$$K = \frac{\rho_*^2(\mathbf{k}_1^2 - \mathbf{k}_2^2)}{\alpha + \rho_*^2 k_{ZF}^2}\, \mathbf{k}_1 \times \mathbf{k}_2 \cdot \mathbf{e}_z , \tag{6}$$

where $\alpha = 1$ for the standard HM equation and $\alpha = 0$ for the modified HM equation. As $\rho_*^2 k_{ZF}^2$ is generally small for ZFs, the coupling constant turns out to be substantially larger for the modified HM model, and this is indeed the reason why ZFs can reach such a large amplitude in that case.

B. Effect of the linear diamagnetic term

In order to assess whether the observed bursts persist in a regime of turbulence dominated by nonlinear effects, we have varied the ratio $\beta \equiv a/L_n$, which determines the relative strength of the linear diamagnetic term compared to the nonlinearity. The results for $\beta = 0$ (flat density profile), 0.3, 0.8, and 2.0 are presented in Fig. 6. For this set of runs, the ZF damping has been set to $\mu_2 = 0.05$, whereas all other parameters are the same as in Sec. III A (see also Table I for a summary of all parameters).

It appears that a small β is very effective in suppressing the large-amplitude oscillations, which are observed only for $\beta = 0.8$ or higher. The period of the oscillations increases slightly with β [Figs. 6(c)–6(d)]. We also notice that the overall level of turbulence increases with β. This is due to the fact that a large diamagnetic term reduces the impact of the nonlinear term by decorrelating the phases of nonlinearly interacting modes. Therefore, the energy injected by the forcing term can pile up for a longer time before being transferred to other modes.[21]

The isotropic spectra of the linear diamagnetic term and the nonlinear term of Eq. (1) (i.e., $i\beta k_x \phi_{\mathbf{k}}$ and the Poisson bracket, respectively) are plotted in Fig. 7. For all cases except $\beta = 0.1$, the linear term dominates for wave numbers $k\rho_* < 1$. We can conclude that the large-amplitude oscillations only appear when the linear term is dominant, although the actual threshold may not be easy to determine. For instance, the case $\beta = 0.6$ still gives rise to no oscillations despite being predominantly linear. Finally, we also point out that ZF production is always intrinsically nonlinear in this model, as the only ZF source term arises through nonlinear coupling of DWs, and the linear ZF term involving the diamagnetic frequency is always zero.

C. Effect of diamagnetic term at lower ρ_*

Finally, we consider a case where the normalized Larmor radius is smaller: $\rho_* = 0.007$, while keeping the same forcing wave number $\rho_* k_0 = 0.7$. The grid size remains $N_x = N_y = 256$, so that the forcing wave number is now closer to the maximum wave number allowed ($\rho_* k_{max} = 0.89$). Therefore, in order to limit the dissipation to scales smaller than the forcing wavelength, we use hyperdiffusion with $p = 4$ and $\mu_1 = 2 \times 10^{-12}$. Other parameters are given in Table I.

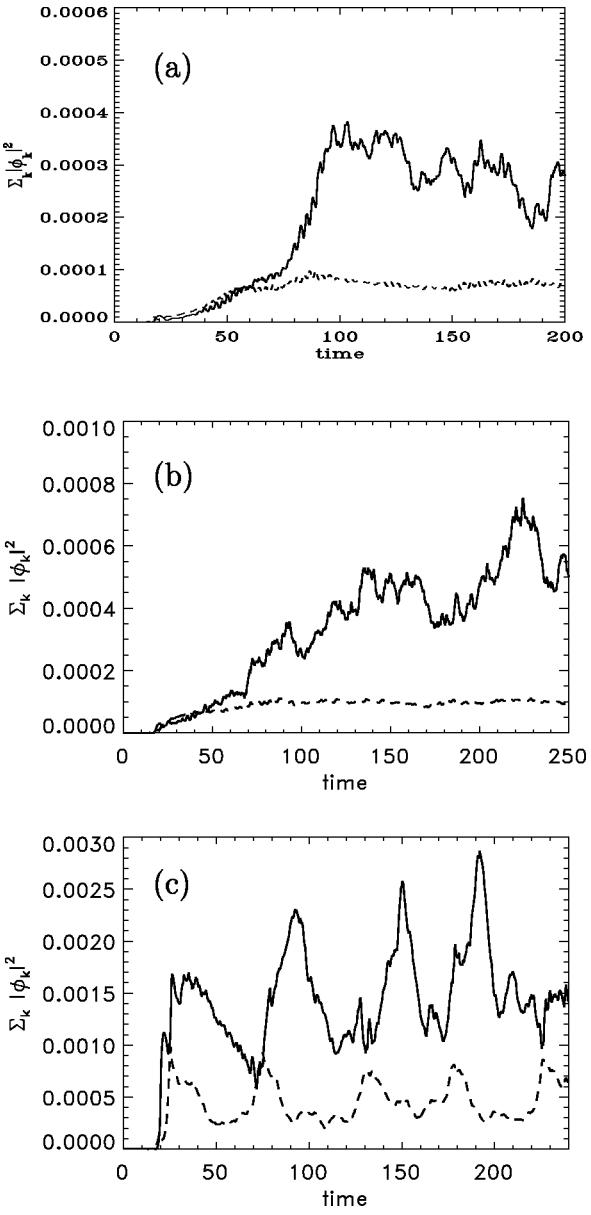

FIG. 8. Time evolution of the ZF (solid line) and DW (dashed line) spectra (Sec. III C), for $\rho_* = 0.007$ and (a) $\beta = 0$, (b) $\beta = 1.0$, and (c) $\beta = 5.0$. For clarity, the DW spectrum in (c) is magnified by a factor 2.

Three runs with different values of the density gradient $\beta = a/L_n$ were performed. Figure 8 shows that the large-amplitude oscillations only appear when β is sufficiently large ($\beta \geqslant 5$), i.e., when the linear diamagnetic term is dominant. The pattern observed in the previous sets of simulations is thus recovered at lower values of the normalized Larmor radius.

IV. CONCLUSION

We have demonstrated that large oscillations in the ZFs can be generated in the simplest nontrivial model of drift wave turbulence, namely a modified Hasegawa–Mima equation. These oscillations appear when the linear diamagnetic term (proportional to the density gradient) dominates over

the nonlinearity. In the opposite case, both ZFs and DWs saturate at a roughly constant level, with no oscillations. Since they are observed in our 2D slab model, such oscillations cannot be due to toroidal, three-dimensional, or kinetic effects. The key ingredient appears to lie in the modified adiabatic electron response, which triggers a significant ZF excitation, as was previously suggested by the analysis of a four-wave model.[11] Indeed, the oscillations were not observed in the standard HM model.

The analysis of the early stages of the simulations revealed that the ZFs grow exponentially with a rate that is twice that of the DWs, independently of other parameters. This fact can be justified by means of a simple model equation, and is due to the quadratic nature of the nonlinearity. We have also found that, in the standard HM model, ZFs saturate at a much lower level compared to the modified HM. This can also be explained in part with a simple argument, showing that the ZF saturation level depends directly on the nonlinear coupling coefficient (which is much larger for the modified HM), and inversely on the dissipation rate.

In summary, we have shown that generation of large-scale structures such as ZFs can be expected even for the simplest model of drift turbulence. As the shearing due to ZFs is known to control the evolution of large-scale radial events,[1,2] the observed oscillatory behavior may be important in generating bursty, nondiffusive transport in experimental devices.

ACKNOWLEDGMENTS

The authors would like to acknowledge useful discussions with Pierre Bertrand, Jack Connor, Bill Dorland, Richard Dendy, Chris Lashmore-Davies, and Chippy Thyagaraja.

This work was jointly funded by the UK Department of Trade and Industry and EURATOM, with additional support from EURATOM mobility funding.

[1] B. N. Rogers, W. Dorland, and M. Kotschenreuther, Phys. Rev. Lett. **85**, 5336 (2000).
[2] P. Beyer, S. Benkadda, X. Garbet, and P. H. Diamond, Phys. Rev. Lett. **85**, 4892 (2000).
[3] S. Benkadda, P. Beyer, N. Bian *et al.*, Nucl. Fusion **41**, 995 (2001).
[4] B. A. Carreras, B. Ph. van Milligen, M. A. Pedrosa *et al.*, Phys. Plasmas **6**, 1885 (1999).
[5] P. A. Politzer, Phys. Rev. Lett. **84**, 1192 (2000).
[6] A. Hasegawa and K. Mima, Phys. Fluids **21**, 87 (1978).
[7] A. I. Smolyakov, P. H. Diamond, and M. Malkov, Phys. Rev. Lett. **84**, 491 (2000).
[8] A. I. Smolyakov, P. H. Diamond, and V. I. Shevchenko, Phys. Plasmas **7**, 1349 (2000).
[9] L. Chen, Z. Lin, and R. White, Phys. Plasmas **7**, 3129 (2000).
[10] P. N. Guzdar, R. G. Kleva and L. Chen, Phys. Plasmas **8**, 459 (2001).
[11] G. Manfredi, C. M. Roach, and R. O. Dendy, Plasma Phys. Controlled Fusion **43**, 825 (2001).
[12] C. N. Lashmore-Davies, A. Thyagaraja, and D. McCarthy, Phys. Plasmas **8**, 5121 (2001).
[13] Z. Lin, T. S. Hahm, W. W. Lee, W. M. Tang, and P. H. Diamond, Phys. Rev. Lett. **83**, 3645 (1999); Z. Lin, T. S. Hahm, W. W. Lee, W. M. Tang, and R. B. White, Phys. Plasmas **7**, 1857 (2000).
[14] M. A. Malkov, P. H. Diamond, and M. N. Rosenbluth, Phys. Plasmas **8**, 5073 (2001).
[15] A. Hasegawa and K. Mima, Phys. Fluids **21**, 87 (1978).
[16] W. Dorland and G. W. Hammett, Phys. Fluids B **5**, 812 (1993).
[17] M. Ottaviani and G. Manfredi, Nucl. Fusion **41**, 637 (2000).
[18] T. H. Stix, Phys. Fluids **16**, 1260 (1973).
[19] G. R. McKee, C. C. Petty, R. E. Waltz *et al.*, Nucl. Fusion **41**, 1235 (2001).
[20] A. M. Dimits, G. Bateman, M. A. Beer *et al.*, Phys. Plasmas **7**, 969 (2000).
[21] G. Manfredi, J. Plasma Phys. **61**, 601 (1999).